GEOLOGY | THE GEOLOGICAL SOCIETY OF AMERICA®

https://doi.org/10.1130/G50665.1

Manuscript received 13 August 2022
Revised manuscript received 23 October 2022
Manuscript accepted 18 November 2022

Published online 9 February 2023

Carbon released by sill intrusion into young sediments measured through scientific drilling

Daniel Lizarralde[1], Andreas Teske[2], Tobias W. Höfig[3], Antonio González-Fernández[4] and the IODP Expedition 385 Scientists*

[1]Department of Geology and Geophysics, Woods Hole Oceanographic Institution, Woods Hole, Massachusetts 02543, USA
[2]Department of Earth, Marine and Environmental Science, University of North Carolina at Chapel Hill, Chapel Hill, North Carolina 27599, USA
[3]International Ocean Discovery Program, Texas A&M University, 1000 Discovery Drive, College Station, Texas 77845, USA
[4]Department of Geology, Centro de Investigación Científica y de Educación Superior de Ensenada (CICESE), 3918 Carretera Ensenada-Tijuana, Ensenada, Baja California 22860, Mexico

ABSTRACT

The intrusion of igneous sills into organic-rich sediments accompanies the emplacement of igneous provinces, continental rifting, and sedimented seafloor spreading. Heat from intruding sills in these settings alters sedimentary organic carbon, releasing methane and other gasses. Recent studies hypothesize that carbon released by this mechanism impacts global climate, particularly during large igneous province emplacements. However, the direct impacts of sill intrusion, including carbon release, remain insufficiently quantified. Here, we present results from International Ocean Discovery Program (IODP) Expedition 385 comparing drill-core and wireline measurements from correlative sedimentary strata at adjacent sites cored in Guaymas Basin, Gulf of California, one altered by a recently intruded sill and one unaffected. We estimate 3.30 Mt of carbon were released due to this sill intrusion, representing an order of magnitude less carbon than inferences from outcrops and modeling would predict. This attenuated carbon release can be attributed to shallow intrusion and the high heat capacity of young, high-porosity sediments. Shallow intrusion also impacts sub-seafloor carbon cycling by disrupting advective fluxes, and it compacts underlying sediments, increasing potential carbon release in response to subsequent intrusions.

INTRODUCTION

Hydrocarbon formation driven by igneous sill intrusion into sedimentary basins has been extensively studied in both field and laboratory settings. Early scientific interest in using the steep thermal gradients surrounding sills as analogs for hydrocarbon maturation with burial (Simoneit et al., 1978) expanded into study of the metamorphic aureole of sills themselves (e.g., Saxby and Stephenson, 1987). The demonstration that sill intrusion in the North Atlantic Ocean basin could plausibly explain rapid early Eocene warming and the associated negative carbon isotope excursion (Svensen et al., 2004) was followed by studies linking these processes to end-Permian extinctions (Svensen et al., 2004; Kaiho et al., 2009), Early Jurassic warming (Svensen et al., 2007), and Cretaceous anoxia (Turgeon and Creaser, 2008). The discovery of sill-hosted hydrothermal systems in Guaymas Basin (Curray et al., 1982), Gulf of California, extended this interest to ecosystems supported by high-temperature alteration products (e.g., Zierenberg and Holland, 2004; Teske et al., 2014) and introduced the notion that processes driven by sill intrusion, including alteration and release of gases out of the seabed, persist through time in many marine settings and are not limited to singular igneous events.

IODP EXPEDITION 385 SITES U1545 AND U1546

International Ocean Discovery Program (IODP) Expedition 385 to Guaymas Basin (Fig. 1) explored the influence of systematic, widespread igneous sill intrusion on carbon cycling in young ocean basins. Guaymas Basin is a marginal basin that transitioned from rifting to seafloor spreading ca. 6 Ma (Lizarralde et al., 2007; Miller and Lizarralde, 2013) and thus has attributes in common with young continental rifts and back-arc basins, including marine and terrestrial sedimentation, high heat flow, and active magmatism. Seismic data show that active magmatism in Guaymas Basin is not confined to the divergent plate boundary, but it instead extends tens of kilometers off axis, where it is manifest as sill intrusions into sediments (Lizarralde et al., 2011). In contrast to on-axis hydrothermalism, off-axis sill magmatism has the potential to impact a much larger volume of sedimentary carbon (Lizarralde et al., 2011) and is analogous to sedimentary basin intrusions implicated in climate perturbations.

A key objective of Expedition 385 was to quantify sill-driven carbon release from off-axis sills. Sites U1545 and U1546 (Fig. 1) were chosen to address this objective by comparison of cores from the two sites, one affected by a massive sill intrusion and one unaffected. The close spacing (~1.1 km) of the sites and the relatively simple stratigraphy enable confident correlation between sites. The sill at Site U1546 is shallow enough to be accessible to scientific drilling, thick enough (~77 m) to have an unambiguous thermal impact, and thin enough to enable coring through the sill and into underlying sediments.

Sites U1545 and U1546 were cored to depths of 503.3 and 540.2 m below seafloor (mbsf), with high core recovery (Teske et al., 2021a, 2021b). The recovered sediments at both sites consist of a mix of biogenic and terrigenous components, primarily siliceous diatom tests, siliciclastic particles, and authigenic carbonate as micrite and nodules. The sediments are mostly laminated, implying limited burrowing and a low-oxygen seafloor environment. Total organic carbon (TOC) measured in core samples decreases from

*International Ocean Discovery Program (IODP), Expedition 385, http://publications.iodp.org/proceedings/385/385title.html

CITATION: Lizarralde, D., et al., 2023, Carbon released by sill intrusion into young sediments measured through scientific drilling: Geology, v. 51, p. 329–333, https://doi.org/10.1130/G50665.1

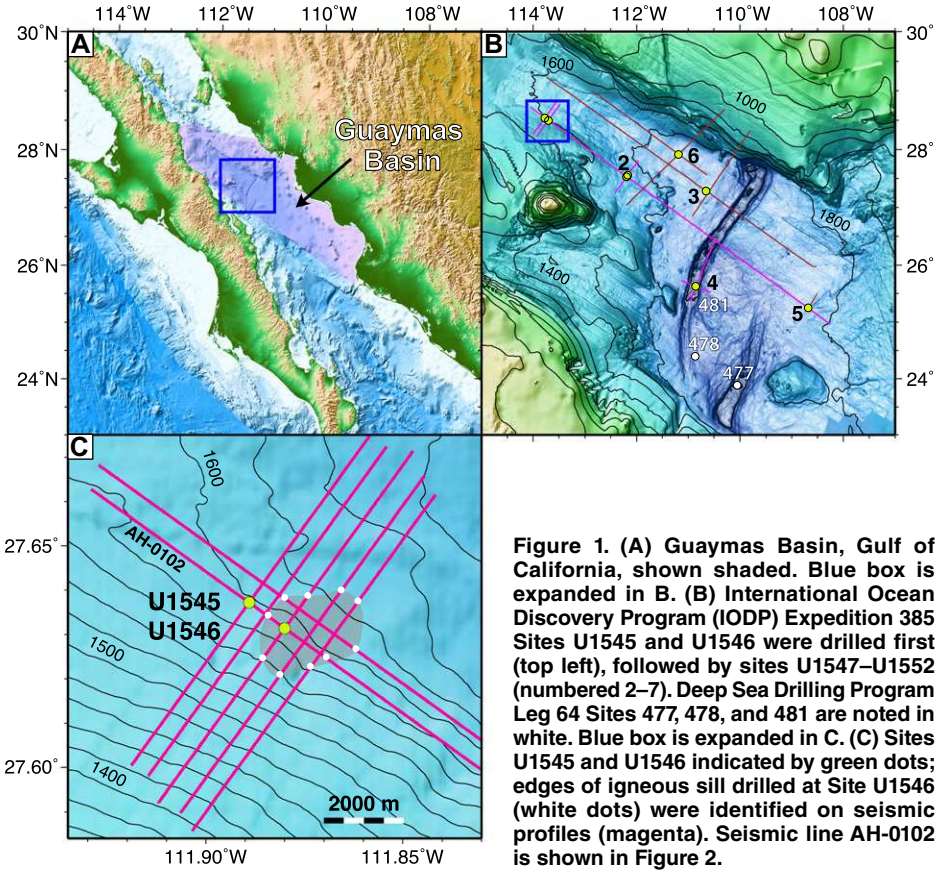

Figure 1. (A) Guaymas Basin, Gulf of California, shown shaded. Blue box is expanded in B. (B) International Ocean Discovery Program (IODP) Expedition 385 Sites U1545 and U1546 were drilled first (top left), followed by sites U1547–U1552 (numbered 2–7). Deep Sea Drilling Program Leg 64 Sites 477, 478, and 481 are noted in white. Blue box is expanded in C. (C) Sites U1545 and U1546 indicated by green dots; edges of igneous sill drilled at Site U1546 (white dots) were identified on seismic profiles (magenta). Seismic line AH-0102 is shown in Figure 2.

~5 wt% at the seafloor to ~2 wt% at 200 mbsf for both sites. Wireline logging measurements at each site, including seismic velocity, natural gamma radiation, and density, enabled accurate depth migration of the seismic profile crossing the sites (Fig. 2); detailed stratigraphic correlation (see the Supplemental Material[1]); and the conversion from wt% TOC to volumetric weight of carbon (Fig. 3).

The 77-m-thick sill cored at Site U1546 is evident in the seismic profile, with a top at ~355 mbsf and notable deformation of the overlying sediments. The entire thickness of the sill was drilled, with 73% core recovery. The stratigraphic correlation between sites indicates that the youngest and oldest possible paleo-seafloor horizons at the time of sill intrusion are marked by horizons Y and 3, respectively, in Figure 2. Biostratigraphic datums identified in cores (Teske et al., 2021a, 2021b) provide a sedimentation rate of ~102 cm/k.y. The sill thus intruded between 76 ka at 277 mbsf and 149 ka at 201 mbsf. In situ formation temperature measurements were made every ~30 m at each site. The observed linear geothermal gradient of ~223 °C/km indicates steady-state heat flow and implies thermal equilibration of the sill. Thus, the temperature of sediment surrounding the sill at the time of intrusion would have been similar to modern values of ~50–65 °C. Core observations of grain sizes and igneous textures suggest that the sill formed from a single magmatic pulse and cooled slowly enough to develop smooth transitions from basaltic to doleritic rock types (Teske et al., 2021b).

The metamorphic aureole of the sill at Site U1546 can be estimated from changes in TOC measured in core samples (Teske et al., 2021a, 2021b) and from the production index (PI) calculated from source-rock analyses (SRA; Teske et al., 2021c). PI, the ratio of free hydrocarbon to free plus cracking-generated hydrocarbon (both measured using SRA; Peters, 1986), enables oil-generation ($0.1 < PI < 0.3$) and gas-generation ($PI > 0.3$) zones to be inferred. PI values for U1546 samples are shown in Figure 3 along with green- and blue-shaded areas indicating the oil- and gas-generation zones inferred from that index. Above the upper aureole, average measured TOC is ~30 kg/m^3 at correlative depths for both sites. Site U1546 values are consistently below that average, and they are also less than correlative U1545 values, beginning at ~16 m above the sill, which corresponds to the top of the oil-generation zone, and they decrease significantly beginning at ~8 m above the sill, similar to the gas-generation zone. Below the sill, average TOC for Site U1546 samples is near 40 kg/m^3 below 455 mbsf, though the TOC of the deepest correlative Site U1545 samples, at ~31 kg/m^3, is similar to values above the sill.

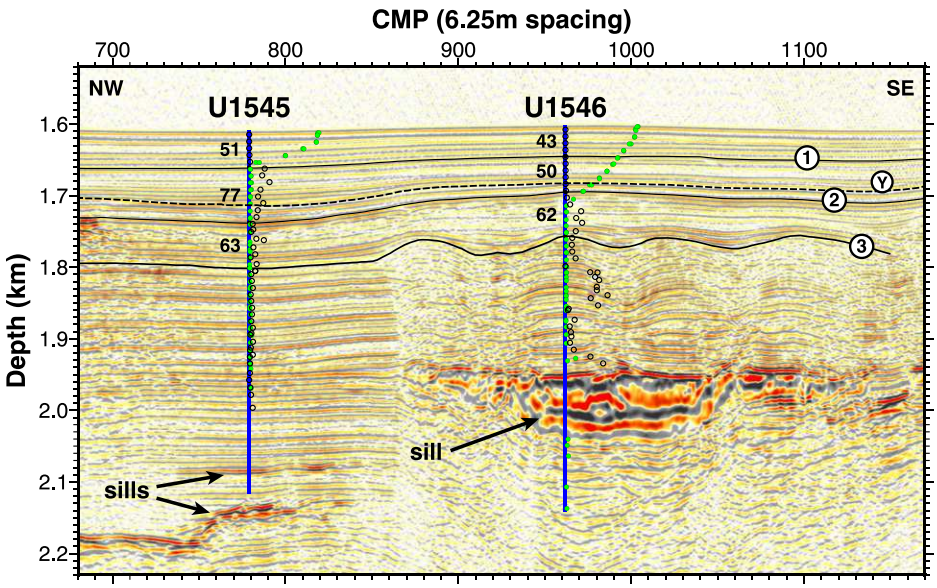

Figure 2. Depth-migrated seismic section AH-0102 crossing International Ocean Discovery Program (IODP) Expedition 385 Sites U1545 and U1546 (Fig. 1C); blue lines indicate total drilled depth (km below sea level). Measured pore-water sulfate (green dots) and headspace methane (open dots) are indicated (see the Supplemental Material [see footnote 1]). Black and dashed lines are seismic sequence boundaries; numbers are sediment thicknesses in meters from seafloor to boundary 1, and between boundaries 1–2 and 2–3; Y marks youngest paleo-seafloor consistent with stratigraphy, and 3 marks oldest. CMP—common midpoint.

[1]Supplemental Material. List of International Ocean Discovery Program (IODP) Expedition 385 co-author scientists; pore-water sulfate and methane profiles for Sites U1545 and U1546; and details of the site-to-site stratigraphic correlation. Please visit https://doi.org/10.1130/GEOL.S.21919353 to access the supplemental material and contact editing@geosociety.org with any questions.

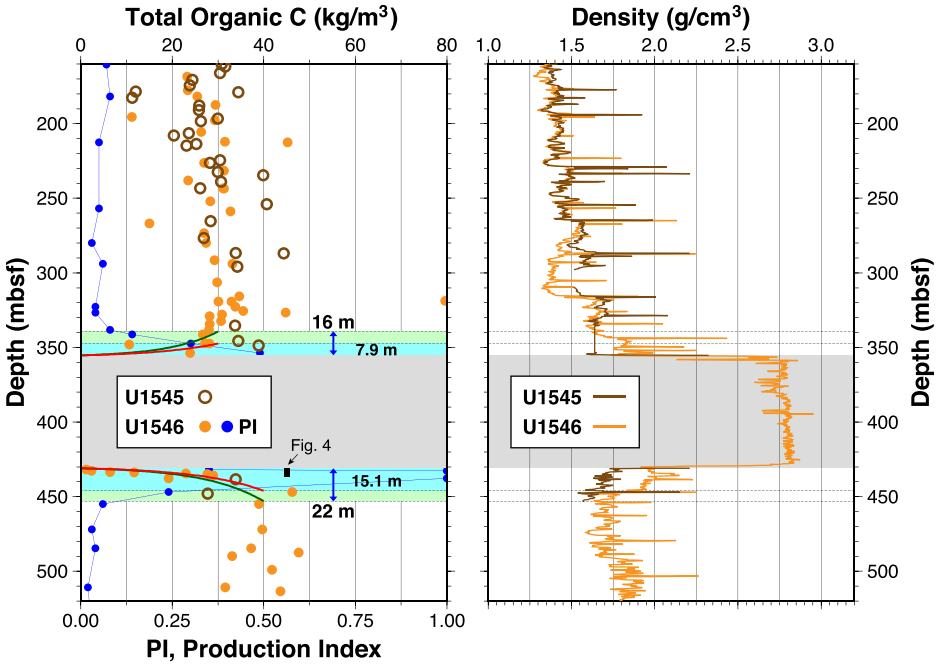

Figure 3. (Left) Total organic carbon (brown dots) measured from core samples as weight percent and converted to density using density logs in right panel. Data from International Ocean Discovery Program (IODP) Expedition 385 Site U1545 were shifted to stratigraphic correlative depths at Site U1546 (see the Supplemental Material [see footnote 1]). Blue dots are production index (PI), where green regions are oil generation, and blue regions are gas generation. Green and red curves are exponential functions integrated to estimate organic carbon present within alteration zone. (Right) Bulk density log profiles from Sites U1545 and U1546, with = U1545 log shifted to depths correlative with U1546. Gap in U1545 log between 336 and 353 mbsf (correlative depth) has been filled with median measured value between 320 and 345 mbsf.

A notable decrease in TOC upward toward the sill base occurs over ~15 m beginning at ~447 mbsf, consistent with the base of the gas-generation zone. The alteration of sediment is visibly evident as color and texture changes in cores from beneath the sill over a depth interval of ~5 m (Fig. 4).

ESTIMATE OF CARBON RELEASED DUE TO SILL INTRUSION

The amount of "released carbon" is understood to be the difference between the amount of organic carbon in sediments before versus after the intrusion and alteration by a sill. Estimating carbon release involves defining the altered zone and subtracting estimates of organic carbon present after intrusion from carbon present before intrusion. The postintrusion case can be confidently estimated based on TOC measurements and SRA performed on sediment core samples from Site U1546 (Teske et al., 2021b, 2021c). The pre-intrusion case can similarly be estimated based on TOC measurements outside of the metamorphic aureole at Site U1546 and comparison with TOC measured in correlative strata from Site U1545 (Fig. 3).

The core-sample measurements of TOC within the aureole indicated a steep decrease toward the sill. We estimated TOC present within the aureole to decrease exponentially toward the sill from a reference value to zero, yielding a release of ~70% of the available organic carbon over a given interval. We considered two cases, one with carbon release from the oil-generation boundary to the sill (gas + oil case) and one from the gas-generation boundary (gas-only case). We used reference values of 30 kg C/m^3 above the sill and 40 kg C/m^3 below the sill. The reference values yielded pre-intrusion organic carbon spatial densities of 1364 kg C/m^2 and 843 kg C/m^2 for the gas + oil and gas-only cases. Subtracting calculated TOC within the aureole yielded spatial densities of 983 kg C/m^2 and 586 kg C/m^2 for the two cases, with an average of 784 kg C/m^2. Multiplying these densities by an estimated 4.2 km^2 area of the sill at Site U1546 (Fig. 1) yielded maximum and minimum amounts released of 4.12 and 2.46 Mt of C, or an average amount of 3.29 Mt of C released due to sill intrusion. This is equivalent to 3.86 Mt of CH_4 or 12.85 Mt of CO_2.

COMPARISON OF MEASURED CARBON RELEASED TO OTHER ESTIMATES

The estimated carbon released linked to the 77-m-thick sill at Site U1546 is substantial, equivalent to about one quarter of the annual global CO_2 flux from terrestrial volcanism (53.1 Mt of CO_2; Fischer et al., 2019). However, our estimate of 3.3 Mt of C is small for an intruded sill of this size relative to computations using published models. Modeling by Aarnes et al. (2010) predicts that a 100-m-thick, 4.2-km^2-area sill intruding sediments with 2 wt% organic carbon would have a methane-generation potential of 73 Mt of CH_4. Iyer et al. (2013) predicted the same sill may release ~109 Mt of CH_4 in models that included fluid flow. The 10-fold difference between these model predictions and observations cannot be due solely to the 25% difference between observed and modeled sill thicknesses. Factors that impact sill-driven gas generation include intrusion depth, host-rock temperature, and sediment type. Models of sills intruded at depths ranging from 0.4 to 5.1 km indicate that intrusion depth is the dominant factor controlling methane mobilization (Galerne and Hasenclever, 2019).

Sill-driven organic matter pyrolysis is increasingly limited as intrusion depth shallows above 500 m. Marine sediment porosity commonly decreases with compaction from ~100% to ~50% over the upper 500 mbsf, with a trend toward more linear decrease below 500 m (Tenzer and Gladkikh, 2014). The volumetric density of organic carbon increases with compaction, while the specific heat of the sediment decreases. Higher-porosity sediments therefore require more heat to raise their temperature, since the heat capacity of water is large, i.e., ~5 times that of sedimentary grains. The difference in aureole thickness above versus below the sill at Site U1546 and the corresponding factor-of-two difference in carbon release are likely due to the influence of compaction. The stratigraphic correlation indicates that ~36 m of sill thickness was accommodated by compaction of underlying sediments, with a corresponding ~12.5% increase in bulk density and an ~39% decrease in heat capacity of the compacted sediments, which is similar to the ~38% difference in aureole thickness below versus above the sill.

Intrusion depth also dictates host-rock temperature for a given geothermal gradient, with deeper intrusions requiring less heat to warm sediment to hydrocarbon-formation temperatures. The thermal gradient at Site U1546 is large, and the temperatures at the ~230 m intrusion depth are similar to those at ~1 + km depth in many continental basins. Therefore, the relative inefficiency of carbon release for the sill at Site U1546 cannot be ascribed to low host-rock temperatures. Similarly, the organic matter within the sediments at Site U1546 consists primarily of type II kerogen (Teske et al., 2021a, 2021b). This would not limit hydrocarbon production given the availability of water to provide hydrogen (Seewald, 2003).

PERSISTENT INFLUENCE OF A SHALLOW INTRUDED SILL

The sill that intruded at Site U1546 appears to have had an impact on carbon cycling within

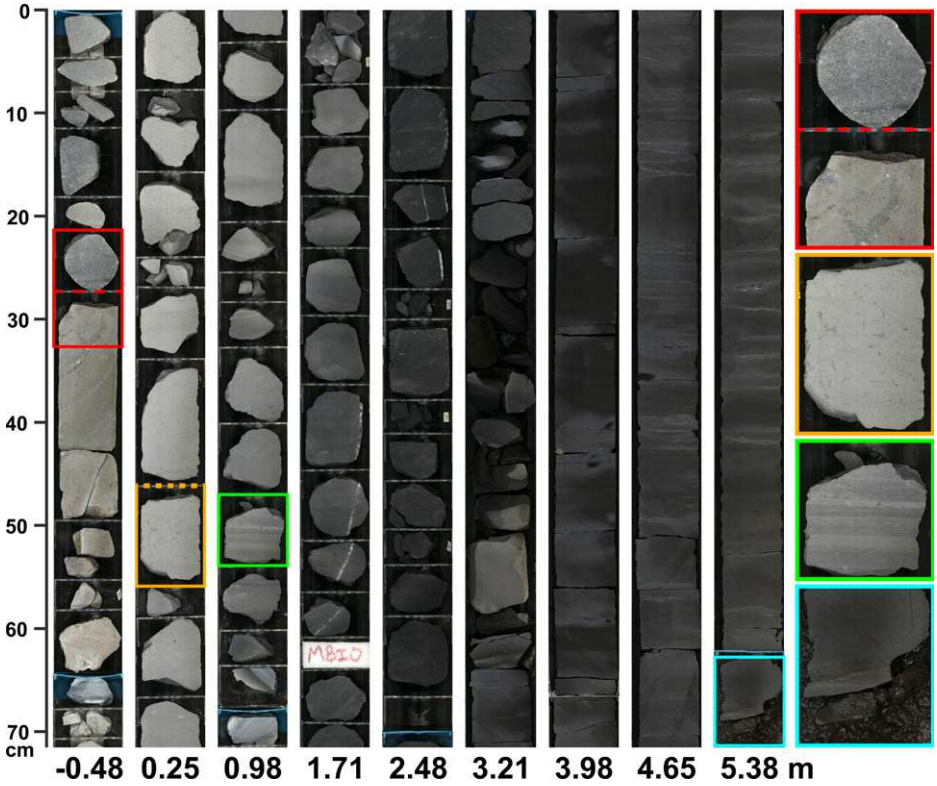

Figure 4. Core sections from International Ocean Discovery Program (IODP) Expedition 385 Site U1546 across sill/sediment transition. Depth scale in cm is shown at left. Numbers below columns are distances (m) below sill/sediment contact (top of orange box). Samples within colored boxes are shown enlarged at right. Red box—doleritic (upper sample) to basaltic (lower) textural transition; orange—indurated sediment from just below sill/sediment contact, with possible sediment/magma mixing; green—laminated chert; blue—dark brown siliceous claystone (with drilling breccia) visually similar to cores from remaining ~100 m cored interval.

the upper 100 m of sediment, distinct from thermogenic alteration, and it persists to the present day. Pore-water sulfate and core-headspace methane concentrations measured from cores (Fig. 2; see the Supplemental Material) indicate a large difference in the depth of the sulfate/methane transition zone (SMTZ) between Sites U1545 (50 mbsf) and U1546 (110 mbsf). The SMTZ marks the intersection of sulfate and methane concentration profiles and represents the depth where the downward flux of sulfate from the water column is balanced by the upward flux of methane from deeper sediments (Iversen et al., 1985). Headspace gas measurements from cores indicate pore-water peaks reach ~10,000 μM H_2S and ~2.25 mM methane accumulation below the SMTZ (Teske et al., 2021a, 2021b), indicating active methanogenic and sulfate-reducing, methane-oxidizing microbial communities at both sites. The steeper sulfate gradient at Site U1545, however, points to a lower flux of methane at Site U1546 relative to Site U1545.

Compaction-driven advective fluid flux provides a plausible explanation for the difference in SMTZ depths between these sites. Advective flux delivers methane to the SMTZ from below and counters downward diffusion of seawater sulfate (Regnier et al., 2011). Vertically advecting fluids at Site U1546 are limited to fluids that are compacted only out of sediments between the seafloor and the igneous sill due to the low permeability of the sill. These sediments are on average older and thus more compacted than the sediment column at Site U1545. Sills with lateral dimensions that are large with respect to emplacement depth may thus limit the export of thermogenic gas out of the sediment column once the sill has cooled.

SUMMARY

Scientific drilling results show that the impact of igneous sill intrusion into young, shallow basins differs from intrusions into older, deeper sedimentary basins. The large water content of young, shallow sediments requires substantial heat to raise sediment temperature to levels required for thermal cracking of kerogen, resulting in less hydrocarbon production for shallower intrusions. In addition, subsidence of a low-permeability igneous sill into compacting underlying sediments may inhibit upward migration of dissolved thermogenic gases. These effects themselves substantially impact the intruded sediments, which are left more compacted and hydrocarbon rich than those prior to intrusion, effectively accelerating the maturation through compaction and heating with burial that is typically observed within deep sedimentary basins unaffected by igneous intrusions.

ACKNOWLEDGMENTS

This research used samples and data provided by the International Ocean Discovery Program (IODP). We sincerely thank the IODP staff and crew of the D/V *JOIDES Resolution,* and we also thank the two manuscript reviewers for thoughtful comments that improved the paper.

REFERENCES CITED

Aarnes, I., Svensen, H., Connolly, J.A.D., and Podladchikov, Y., 2010, How contact metamorphism can trigger global climate changes: Modeling gas generation around igneous sills in sedimentary basins: Geochimica et Cosmochimica Acta, v. 74, p. 7179–7195, https://doi.org/10.1016/j.gca.2010.09.011.

Curray, J.R., et al., 1982, Initial Reports of the Deep Sea Drilling Project 64: Washington, D.C., U.S. Government Printing Office, 1313 p. https://doi.org/10.2973/dsdp.proc.64.1982.

Fischer, T.P., et al., 2019, The emissions of CO_2 and other volatiles from the world's subaerial volcanoes: Scientific Reports, v. 9, 18716, https://doi.org/10.1038/s41598-019-54682-1.

Galerne, C.Y., and Hasenclever, J., 2019, Distinct degassing pulses during magma invasion in the stratified Karoo basin—New insights from hydrothermal flow modeling: Geochemistry, Geophysics, Geosystems, v. 20, p. 2955–2984, https://doi.org/10.1029/2018GC008120.

Iversen, N., Jorgensen, B.B., and Barker, B., 1985, Anaerobic methane oxidation rates at the sulfate-methane transition in marine sediments from Kattegat and Skagerrak (Denmark): Limnology and Oceanography, v. 30, p. 944–955, https://doi.org/10.4319/lo.1985.30.5.0944.

Iyer, K.L., Rüpke, L., and Galerne, C.Y., 2013, Modeling fluid flow in sedimentary basins with sill intrusions: Implications for hydrothermal venting and climate change: Geochemistry, Geophysics, Geosystems, v. 14, p. 5244–5262, https://doi.org/10.1002/2013GC005012.

Lizarralde, D., et al., 2007, Variation in styles of rifting in the Gulf of California: Nature, v. 448, p. 466–469, https://doi.org/10.1038/nature06035.

Lizarralde, D., Soule, S.A., Seewald, J.S., and Proskurowski, G., 2011, Carbon release by off-axis magmatism in a young sedimented spreading centre: Nature Geoscience, v. 4, p. 50–54, https://doi.org/10.1038/ngeo1006.

Miller, N.C., and Lizarralde, D., 2013, Thick evaporites and early rifting in the Guaymas Basin, Gulf of California: Geology, v. 41, p. 283–286, https://doi.org/10.1130/G33747.1.

Peters, K.E., 1986, Guidelines for evaluating petroleum source rock using programmed pyrolysis: American Association of Petroleum Geologists Bulletin, v. 70, p. 318–329, https://doi.org/10.1306/94885688-1704-11D7-8645000102C1865D.

Regnier, P., Dale, A.W., Arndt, S., LaRowe, D.E., Mogollón, J., and Van Cappellen, P., 2011, Quantitative analysis of anaerobic oxidation of methane (AOM) in marine sediments: A modeling perspective: Earth-Science Reviews, v. 106, p. 105–130, https://doi.org/10.1016/j.earscirev.2011.01.002.

Saxby, J.D., and Stephenson, L.C., 1987, Effect of an igneous intrusion on oil shale at Rundle (Australia): Chemical Geology, v. 63, p. 1–16, https://doi.org/10.1016/0009-2541(87)90068-4.

Seewald, J.S., 2003, Organic-inorganic interactions in petroleum-producing sedimentary basins: Na-

ture, v. 426, p. 327–333, https://doi.org/10.1038/nature02132.
Simoneit, D., Brenner, S., Peters, K.E., and Kaplan, I.R., 1978, Thermal alteration of Cretaceous black shale by basaltic intrusions in the eastern Atlantic: Nature, v. 273, p. 501–504, https://doi.org/10.1038/273501a0.
Svensen, H., Planke, S., Malthe-Sørenssen, A., Jamtveit, B., Myklebust, R., Eidem, T.R., and Rey, S.S., 2004, Release of methane from a volcanic basin as a mechanism for initial Eocene global warming: Nature, v. 429, p. 542–545, https://doi.org/10.1038/nature02566.
Svensen, H., Planke, S., Chevallier, L., Malthe-Sørenssen, A., Corfu, F., and Jamtveit, B., 2007, Hydrothermal venting of greenhouse gases triggering Early Jurassic global warming: Earth and Planetary Science Letters, v. 256, p. 554–566, https://doi.org/10.1016/j.epsl.2007.02.013.
Tenzer, R., and Gladkikh, V., 2014, Assessment of density variations of marine sediments with ocean and sediment depths: Scientific World Journal, v. 2014, https://doi.org/10.1155/2014/823296.
Teske, A., Callaghan, A.V., and LaRowe, D.E., 2014, Biosphere frontiers of subsurface life in the sedimented hydrothermal system of Guaymas Basin: Frontiers in Microbiology, v. 5, https://doi.org/10.3389/fmicb.2014.00362.
Teske, A., Lizarralde, D., Höfig, T.W., and the IODP Expedition 385 Scientists, 2021a, Site U1545, *in* Teske, A., et al., eds., Proceedings of the International Ocean Discovery Program, Expedition Reports, 385: College Station, Texas, International Ocean Discovery Program, https://doi.org/10.14379/iodp.proc.385.103.2021.
Teske, A., Lizarralde, D., Höfig, T.W., and the IODP Expedition 385 Scientists, 2021b, Site U1546, *in* Teske, A., et al., eds., Proceedings of the International Ocean Discovery Program, Expedition Reports, 385: College Station, Texas, International Ocean Discovery Program, https://doi.org/10.14379/iodp.proc.385.104.2021.
Teske, A., Lizarralde, D., Höfig, T.W., and the IODP Expedition 385 Scientists, 2021c, Methods, *in* Teske, A., et al., eds., Proceedings of the International Ocean Discovery Program, Expedition Reports, 385: College Station, Texas, International Ocean Discovery Program, https://doi.org/10.14379/iodp.proc.385.102.2021.
Turgeon, S.C., and Creaser, R.A., 2008, Cretaceous oceanic anoxic event 2 triggered by a massive magmatic episode: Nature, v. 454, p. 323–326, https://doi.org/10.1038/nature07076.
Zierenberg, R.A., and Holland, M.E., 2004, Sedimented ridges as a laboratory for exploring the subsurface biosphere, *in* Wilcock, W.S.D., et al., eds., The Subseafloor Biosphere at Mid-Ocean Ridges: American Geophysical Union Geophysical Monograph 144, p. 305–323, https://doi.org/10.1029/144GM19.

Printed in USA